Development of a multiplex fast-scan system for ultrafast time-resolved spectroscopy

Atsushi Yabushita, Yu-Hsien Lee, and Takayoshi Kobayashi

Articles you may be interested in

Construction and development of a time-resolved x-ray magnetic circular dichroism–photoelectron emission microscopy system using femtosecond laser pulses at BL25SU SPring-8
Rev. Sci. Instrum. **79**, 063903 (2008); 10.1063/1.2937648

Time-resolved momentum imaging system for molecular dynamics studies using a tabletop ultrafast extreme-ultraviolet light source
Rev. Sci. Instrum. **79**, 063102 (2008); 10.1063/1.2930869

Femtosecond time-resolved optical pump-probe spectroscopy at kilohertz-scan-rates over nanosecond-time-delays without mechanical delay line
Appl. Phys. Lett. **88**, 041117 (2006); 10.1063/1.2167812

Picosecond time-resolved electronic spectroscopy in plate impact shock experiments: Experimental development
Rev. Sci. Instrum. **70**, 1743 (1999); 10.1063/1.1149662

Developments of widely tunable light sources for picosecond time-resolved resonance Raman spectroscopy
Rev. Sci. Instrum. **68**, 4001 (1997); 10.1063/1.1148373

Development of a multiplex fast-scan system for ultrafast time-resolved spectroscopy

Atsushi Yabushita,[1] Yu-Hsien Lee,[1] and Takayoshi Kobayashi[1,2]

[1]*Department of Electrophysics, National Chiao-Tung University, Hsinchu 300, Taiwan*
[2]*Department of Applied Physics and Chemistry and Institute for Laser Science,
University of Electro-Communications, 1-5-1 Chofugaoka, Chofu, Tokyo 182-8585, Japan;
International Cooperative Research Project (ICORP), Japan Science and Technology Agency (JST),
4-1-8 Honcho, Kawaguchi, Saitama 332-0012, Japan; and Institute of Laser Engineering,
Osaka University, 2-6 Yamada-oka, Suita, Osaka 565-0971, Japan*

A fast-scan method was developed to obtain time-resolved signals with femtosecond resolution over a picosecond range on the fly and in real time. Traditional fast-scan methods collect data at each probe wavelength one by one, which is time consuming and thus not possible for the study of photofragile materials. In this work, we have developed a system that performs fast scans with multiplex detection. Ultrafast time-resolved spectroscopy was demonstrated using the newly developed system. Femtosecond laser pulses have been used for pump-probe studies of ultrafast processes in various materials, and both electronic relaxation and vibrational dynamics have been studied. However, experiments have been limited in sensitivity and reliability because they are affected by the long-term instability of the ultrashort laser pulses and by the fragility of the samples. The instability of the sources hinders precise determination of electronic decay dynamics and introduces systematic errors. The fragility of the samples reduces their amount or concentration, and can lead to contamination of the materials even if they were pure before the measurement. These effects make it difficult to obtain reproducible and reliable experimental data. In the present work, we have developed a fast-scan pump-probe spectroscopic system that can complete a set of measurements in less than 2 min. Quantitative estimates of the signal reproducibility demonstrate that these measurements provide higher reproducibility and reliability than conventional measurements. © *2010 American Institute of Physics.* [doi:10.1063/1.3455809]

I. INTRODUCTION

Time-resolved studies have been performed using a scanning optical delay line with a motorized stage. They have elucidated the ultrafast dynamics of various materials. In such studies, a lock-in amplifier (LIA) is typically used to improve the signal quality. But a LIA has several problems, including base-band detection and $1/f$ noise, the time required for data acquisition, and modulation of the laser fluence incident on the sample. Fast-scan acquisition of the signals could solve these problems by collecting data on the fly and in real time.[1] However, spectroscopic studies require measurement at each probe wavelength. Such iterative measurements are time consuming, and laser damage accumulates on the sample. As a result, the sample condition at the last probe wavelength can be considerably different from that at the first probe wavelength. To overcome that drawback, we have developed a new fast-scan system with multiplex detection. As an example of the application of this method, we use it to perform femtosecond time-resolved spectroscopy.

Ultrafast spectroscopy is a powerful method for investigating photochemical, photophysical, and photobiological processes. Photochemistry of various reactions has been studied, including isomerization, proton transfer, and electron transfer. Photophysical processes have been measured for carrier dynamics and nonlinear excitations. Photobiological processes have been clarified in vision and photosynthesis.[2–4] Ultrafast spectroscopy also has various important applications to photosensors,[5–7] ultrafast optical switches,[8–10] and ultrafast optical memories.[11–13]

Following the development of femtosecond lasers, ultrafast spectroscopy blossomed[14–17] and expanded into areas such as plasma diagnosis and *in situ* probes for laser manufacturing. Subsequent development of sub-10-fs laser pulses[18–23] elucidated the ultrafast dynamics[24–28] of electronic relaxations and molecular vibrations. After the development of the noncollinear optical parametric amplifier (NOPA),[29,30] ultrafast spectroscopy could be performed across wide spectral regions because its structure is broadband and smooth. The resulting observation of real-time molecular vibrations has provided information about changes in molecular structure during relaxation processes such as internal conversion and intersystem crossing, and chemical reactions including *cis-trans* and *trans-cis* isomerization, proton transfer, and oxidation.[28,31–37]

However, it has been difficult to obtain reproducible results for molecular vibrational modes across long time scales

of several hundred femtoseconds. The difficulty stems mainly from (i) accumulated damage to the samples and (ii) long-term instabilities in the laser intensity.

In conventional ultrafast pump-probe measurements, the delay time is scanned in fine steps (less than several femtoseconds) across a long time span (up to a few tens of picoseconds) in order to observe molecular vibrational signals along with the electronic dynamics. The relaxation and dynamics of molecular vibrational modes can be studied by observing changes in the instantaneous frequencies of the modes associated with corresponding electronic states. Therefore it is necessary to have both a long time range to follow the reactions and a sufficiently short time step to resolve the molecular vibrations whose frequencies change during the electronic processes. One complete scan can take 1 h or more. If the sample is chemically sensitive to radiation, it can be damaged during a single scan. The accumulation of damage, which can be significant when the measurement time is long, makes it difficult to observe the intrinsic dynamics of a sample.

Molecular vibrational periods are on the order of several tens of femtoseconds, observed as a modulation of the ΔA trace in a pump-probe measurement during accumulation of about 100 laser shots at each delay-time step. The intensity of the ultrashort laser pulses, used for generating high order nonlinear effects, is affected by small fluctuations in the temperature, humidity, and airflow around the system. These small disturbances cause instabilities in the laser intensity, which make it difficult to observe the ΔA modulation, because both modulations have roughly the same period of several minutes.

In the present work, we have developed a fast-scan pump-probe system with a multichannel lock-in amplifier (MLA) for multiplex detection. This new method, which we dub "fast-scan pump-probe spectroscopy," improves the reproducibility and reliability of the experimental data. For comparison, conventional pump-probe measurements are first performed for a conjugate polymer film. The data are found to be limited in sensitivity and reliability because they are affected by instabilities in the light source and by the fragility of the samples. When the pulse duration is kept below 10 fs, which is shorter than typical molecular vibrational periods, it is difficult to maintain the long term stability of the laser, hindering determination of the decay dynamics of the electronic states and introducing systematic errors. The fragility of the samples reduces the amount and concentration of the samples and can cause contamination of the materials. These effects make it difficult to obtain reproducible and reliable data. But the experimental data are strikingly improved by using the fast-scan pump-probe spectroscopic system.

II. EXPERIMENT

A. NOPA

We built a NOPA to generate visible laser light whose spectral width is broad enough to generate sub-10-fs pulses for ultrafast time-resolved spectroscopy. Details of the NOPA are presented in Appendix A. The smooth spectral
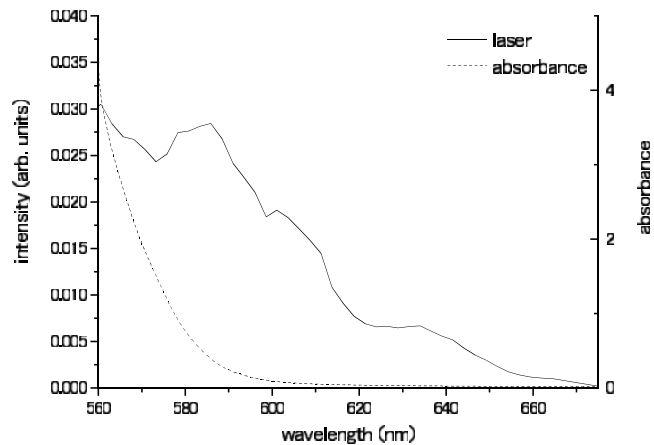

FIG. 1. Incident laser spectrum and absorption spectrum of a sample film.

shape of its output makes it ideal for spectroscopy. The pump source of the NOPA consists of a regenerative chirped pulse amplifier (Legend-USP-HE from Coherent) seeded with a Ti: sapphire laser oscillator (Micra 10 from Coherent). The amplifier generated femtosecond pulses whose duration, central wavelength, repetition rate, and average power were 40 fs, 800 nm, 5 kHz, and 500 mW, respectively. Each pulse from the regenerative amplifier was separated into two pulses by a beam sampler. The larger intensity pulse was used for second harmonic generation (SHG) centered at 400 nm which pumped the NOPA. The other pulse (with ten times weaker intensity) was focused onto a sapphire plate to generate white light by self-phase modulation, to be used as a seed beam for the NOPA. The resulting broadband visible output spectrum plotted in Fig. 1 extends from 530 (18 868 cm^{-1}) to 740 nm (13 514 cm^{-1}) with constant phase. A beamsplitter separated the pump and probe pulses, whose intensities were adjusted using a variable neutral density filter. The energies of the pump and probe pulses were 1 and 0.2 nJ, respectively. Using a beam compressor consisting of a diffraction grating telescopic dispersion line, multilayer dielectric chirped mirrors, and a computer-controlled flexible mirror, the broadband visible laser pulse was compressed to a 10 fs duration before it arrived at the sample surface. The probe pulse was dispersed by a polychromator (SP2300i from Princeton Instruments) into a fiber bundle, the other end of which was separated into 128 fibers connected to avalanche photodiodes (APDs). The time-resolved transmittance difference ΔT of these 128 probe wavelengths was simultaneously detected. The signals were then sent to a MLA with a high signal-to-noise ratio.

B. Mechanical stage for conventional pump-probe measurements

1. Step-scan method

To evaluate our new technique, we compared it to a pump-probe signal obtained using a conventional method. A signal was collected by recording ΔA while scanning the delay time between the pump and probe pulses across a range of -300 to 1500 fs in 0.6 fs steps. For analysis purposes, data with 3 fs steps were obtained by averaging sets of five data points together to suppress artifacts due to interfer-

ence between the pump and probe pulses. The stage used for the step scan (PFS-1020 from Sigma-Tech) had 10 nm (1/15 fs) resolution with full closed-loop control. The positioning resolution was sufficient for ultrafast time-resolved spectroscopy because the time resolution was limited by the duration of the pump and probe pulses. However, the stage required about 600 ms to stabilize between movements, so that a single scan of the pump-probe measurement required at least 30 min.

C. Mechanical stage for novel pump-probe measurements: Fast-scan method

In our new method, the ΔA signal is recorded while scanning the delay time rapidly in 500 steps across a range of 1790 fs. The fast-scan stage (ScanDelay-15 from APE-Berlin) was controlled by an external voltage generated by a digital/analog converter (LPC-361316 from Interface), scanning from -0.2 to $+0.8$ V in 5 s, which is 360 times faster than the 30 min scans of the conventional method. At each delay point, ΔA was obtained in 10 ms, storing the data in the memory of a MLA. Average values were calculated for the data in sets of 24 scans to maintain a good signal-to-noise ratio. Therefore, the measurement time for a single run was 2 min (5×24 s). One can thereby avoid laser fluctuations having correlation times longer than that.

III. RESULTS AND DISCUSSION

The experimental setup, consisting of the NOPA, step-scan stage, and fast-scan stage is shown in Fig. 2(a).

A. Calibration of the delay positions of the fast-scan stage

A 20-μm-thick β-barium borate crystal on a fused silica base plate was used to generate an autocorrelation signal from the broadband spectral width of the laser pulse. While scanning the fast-scan stage, the autocorrelation signal was monitored by a photomultiplier tube (H9656–04 from Hamamatsu) connected to the last channel of the MLA system. As the step-scan stage moves, the autocorrelation signal on the fast-scan trace shifts with the same amount of delay. From the shift, the delay position of the fast-scan trace could be calibrated. The autocorrelation traces were obtained by changing the delay position of the step-scan stage in 50 fs steps. The peak positions of the autocorrelation signal are plotted in Fig. 2(b), giving a calibration curve showing a linear relationship between the delay time and data points of 3.58 ± 0.01 fs/point.

B. Pump-probe measurements using the step-scan method

Pump-probe measurements of a conjugated polymer film were performed by the step-scan method. The preparation of the sample film is detailed in Appendix B. The absorbance change ΔA in the wavelength region from 515 to 753 nm in 2.5 nm steps was obtained by scanning the delay time from -318 to 1482 fs in 0.6 fs steps (forward scan). For each delay point, ΔA was obtained by accumulating for 0.6 s. The mean ΔA spectra in 3 fs steps are shown in Fig. 3(a) in
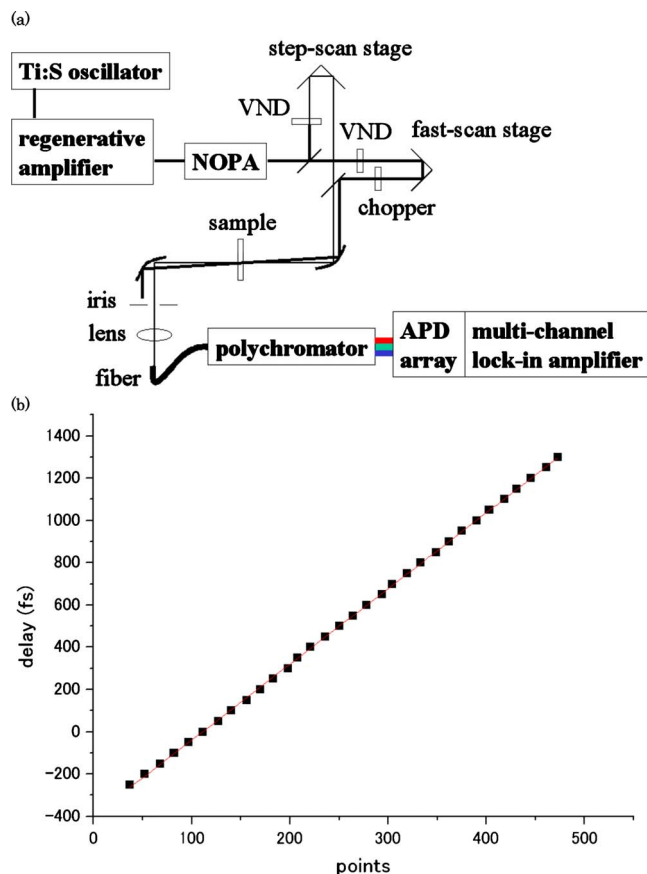

FIG. 2. (Color online) (a) Experimental setup showing the NOPA: noncollinear optical parametric amplifier, VND: variable neutral density filter, and APD: avalanche photodiode. (b) Calibration data for the fast-scan stage (squares) and a linear fit to the data (solid line).

two-dimensional (2D) form. The data in Fig. 3(b) are for the corresponding backward scan. The poor reproducibility between Figs. 3(a) and 3(b) is indicative of sample damage and laser intensity instabilities.

The 2D traces give time-resolved ΔA spectra along their cross sections. The ΔA spectra at three delays (147, 326, and 1221 fs) are plotted in Figs. 3(c) and 3(d) for forward and backward scans, respectively. Damage accumulated in the sample causes scattering, which decreases ΔA in panel (d) compared to that in panel (c).

Time-resolved ΔA traces at three probe wavelengths (568, 575, and 616 nm) were also extracted from the 2D traces in Figs. 3(a) and 3(b) and plotted in panels (e) and (f). In the forward scans, the time-resolved traces start around $\Delta A=0$ for negative delays. In contrast, there exists a large offset at negative delays for the backward scans. The offset is due to damage accumulated on the sample during the step-scan measurements.

Fourier power spectra of the ΔA traces reveal molecular vibrational modes of the sample. Figures 4(a) and 4(b) are the 2D results for forward and backward scans, respectively. They show strong peaks around 1588 cm^{-1}, corresponding to the most intense Raman mode (see Fig. 2 of Ref. 38). However, they have low reproducibility between the forward and backward scans and are not identical in shape with Raman spectra because of the instability of the laser source.
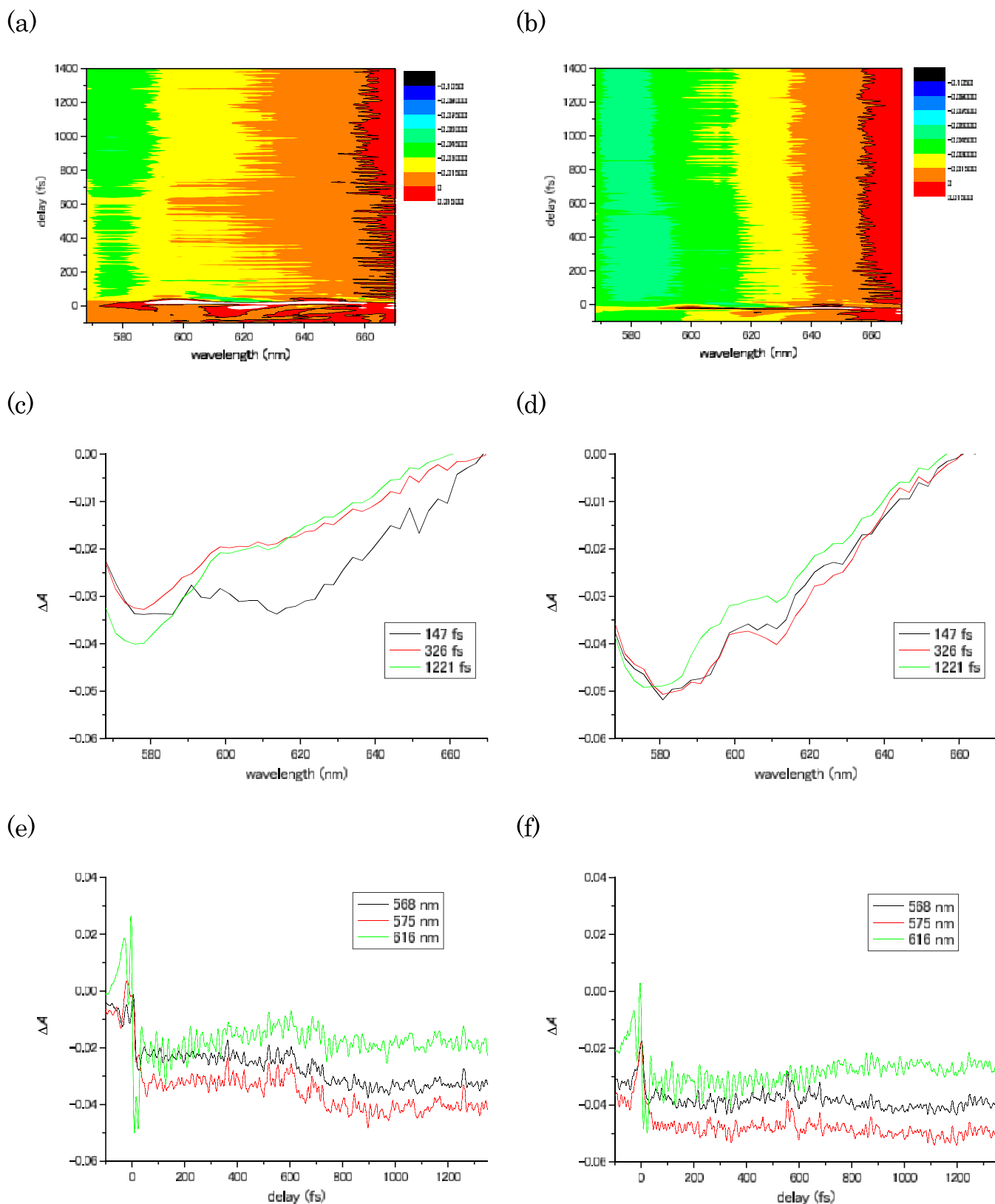
FIG. 3. (Color online) Absorption changes obtained by the step-scan method for delay times of (a) −318 to 1482 fs and (b) 1482 to −318 fs. Time-resolved ΔA spectra at delays of 147, 326, and 1221 fs are plotted in (c) and (d), and ΔA traces at 568, 575, and 616 nm are plotted in (e) and (f).

Fourier power spectra probed at 616 nm were extracted from Figs. 4(a) and 4(b) and plotted in panels (c) and (d). Irreproducibility of the step-scan data can be seen. Figures 4(e) and 4(f) are Fourier power spectra of the most promi-

nent mode at 1588 cm^{-1}, corresponding to the C$=$C stretching mode. They also lack reproducibility.

To study the dynamics of the molecular vibrational modes, a spectrographic analysis was performed. Spectro-
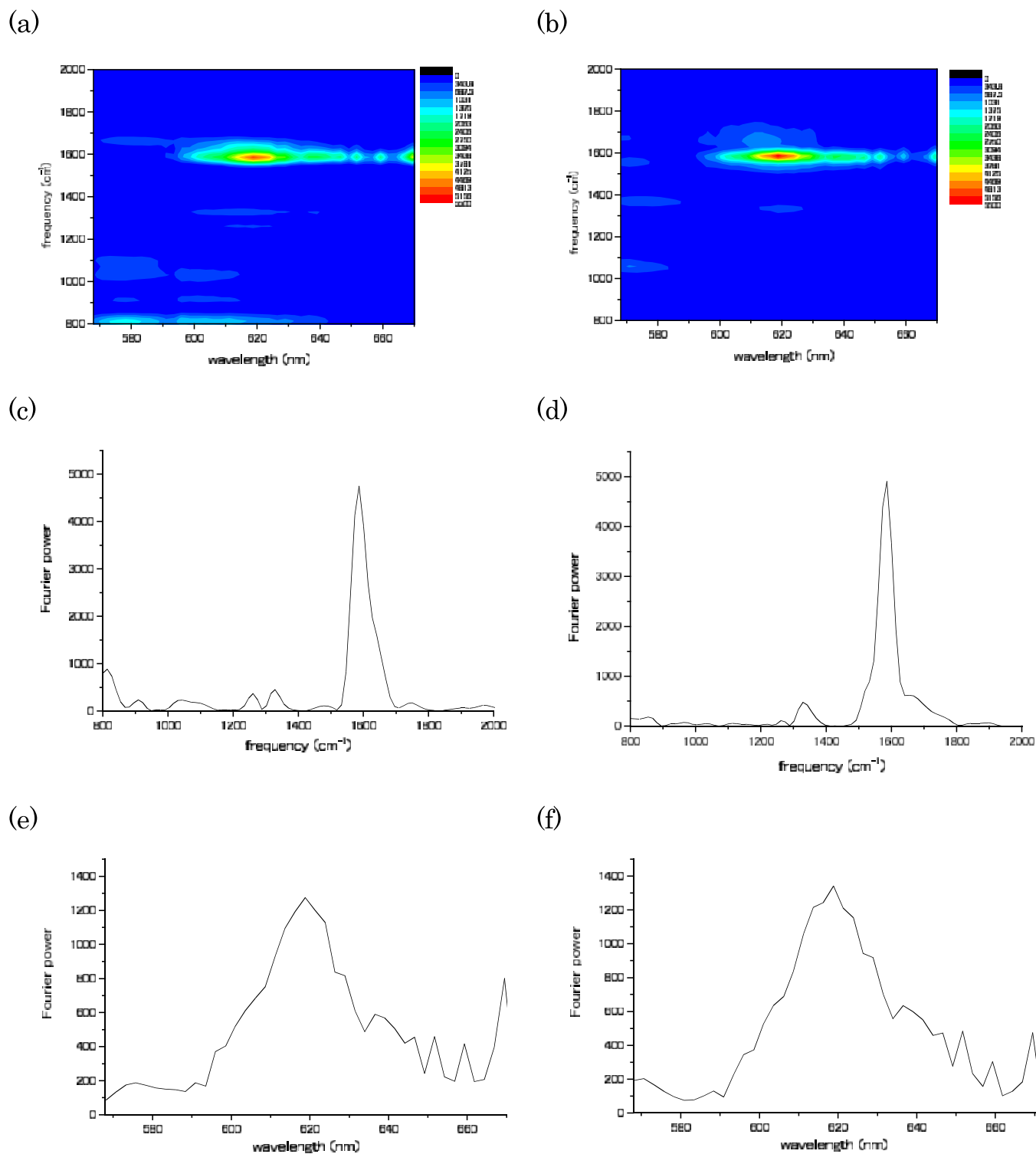
(a)

(b)

(c)

(d)

(e)

(f)

FIG. 4. (Color online) (a) and (b) are Fourier power spectra of the ΔA traces from Figs. 3(a) and 3(b), respectively. Fourier power spectra at 616 nm are plotted in (c) and (d). Fourier power spectra of the most prominent vibrational mode at 1588 cm^{-1} are graphed in (e) and (f).

grams were obtained by a sliding-window Fourier transform using the Blackman window function,

$$S(\omega, \tau) = \int_0^\infty S(t)g(t-\tau)\exp(-i\omega t)dt,$$

$$g(t) = 0.42 - 0.5\cos(2\pi t/T) + 0.08\cos(4\pi t/T),$$

where τ is the gate width, which we set to 600 fs,

corresponding to a full width at half maximum (FWHM) of 240 fs. The calculation of the spectrogram was performed after applying a high-pass filter to the signal because slow modulations of the signal (slower than tens of femtoseconds) arise from fluctuations in the laser power. For forward and backward scans, the results are shown in Figs. 5(a) and 5(b), respectively, using a time-resolved ΔA trace probed at 616 nm. They again show poor reproducibility.
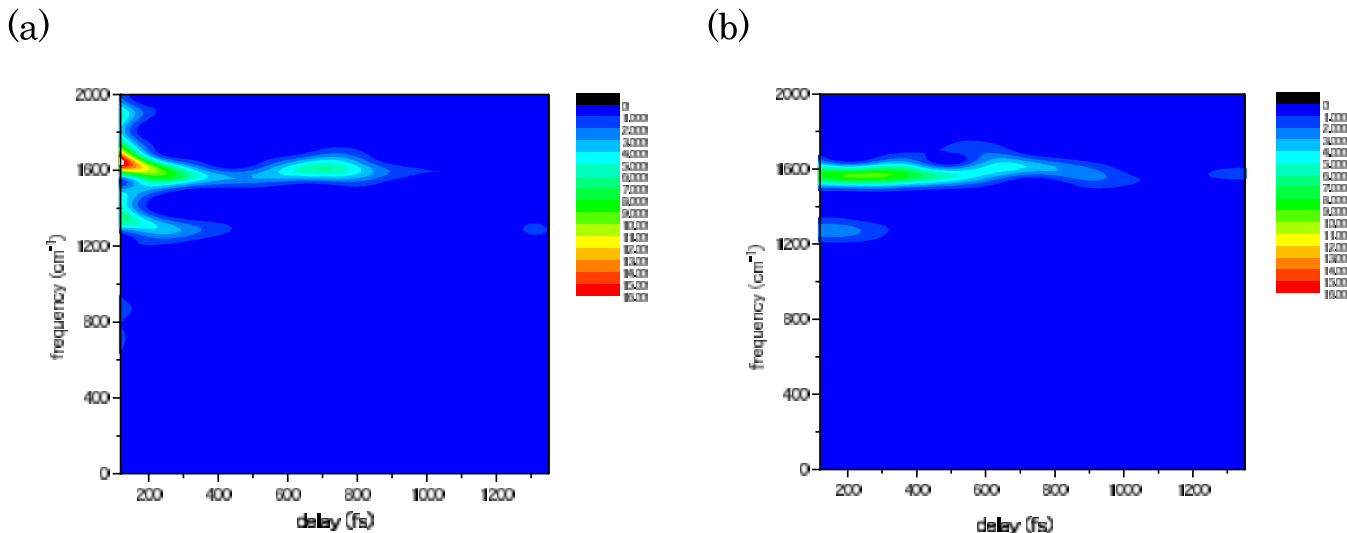
(a)

(b)

FIG. 5. (Color online) (a) and (b) Spectrograms calculated from the time-resolved traces at 616 nm shown in Figs. 3(e) and 3(f).

C. Pump-probe measurements using the fast-scan method

After the preceding step-scan measurements, we moved the sample position to avoid the damaged area and began fast-scan measurements so that the experimental conditions remained identical. Twenty-four forward scans were obtained from −390 to 1396 fs. The mean of the 24 traces is plotted in Fig. 6(a), and backward scanned data from 1396 to −390 fs are shown in Fig. 6(b). In contrast to the step-scan results, these data show high reproducibility.

Figures 6(c) and 6(d) are time-resolved ΔA spectra for the forward and backward scans, respectively, at delays of 147, 326, and 1221 fs. Time-resolved ΔA traces probed at three wavelengths (568, 575, and 616 nm) are plotted for the forward and backward scans in Figs. 6(e) and 6(f), respectively. The improvement in the signal reproducibility was estimated by calculating a correlation coefficient between the time traces for the forward and backward scans from 150 to 1350 fs. Figure 6(g) shows the resulting correlation coefficients for the step-scan and fast-scan measurements. One can see that the reproducibility is much higher in the fast-scan measurements than in the step-scan measurements.

Fourier power spectra of the ΔA traces for the forward and backward scans were calculated and are plotted in Figs. 7(a) and 7(b), respectively. Similar to Figs. 4(c) and 4(d), ΔA traces probed at 616 nm are plotted in Figs. 7(c) and 7(d) for forward and backward scans, respectively. They confirm the reproducibility of the Fourier power spectra and show good agreement with Raman spectra from previous work.[38] Figures 7(e) and 7(f) are Fourier power spectra of the most prominent vibrational mode at 1588 cm^{-1}. Some small differences are evident at wavelengths longer than 640 nm. The small amplitude of ΔA in that spectral region [see Figs. 6(a) and 6(b)] is probably the origin of the error.

Between 600 and 640 nm, where the Fourier power is high, the signal reproducibility was quantified by calculating the error in the determination of the power for molecular vibrational modes of 963, 1112, 1261, 1316, and 1587 cm^{-1}. The relative difference in the Fourier power of a forward

scan (I_f) and a backward scan (I_b) is $|(I_f - I_b)/(I_f + I_b)|$. Figures 7(g) and 7(h) shows the errors calculated for step-scan and fast-scan measurements, respectively. Evidently the Fourier power can be determined more precisely for the latter.

Using a Blackman gate with a FWHM of 240 fs, spectrograms were calculated for the time-resolved traces obtained in the fast-scan measurement. The results are plotted in Figs. 8(a) and 8(b) for the forward and backward scans, respectively, and show good reproducibility. Therefore, the fast-scan method is preferable not only for the study of electronic dynamics but also for the study of vibrational dynamics.

IV. SUMMARY

The fast-scan method obtains time-resolved signals with femtosecond resolution over a picosecond range on the fly and in real time. However, it is traditional in time-resolved spectroscopy to measure data at each probe wavelength one by one, which is time consuming and results in damage accumulation on a sample.

In this paper we reported a new fast-scan system with multiplex detection. It is particularly useful for ultrafast spectroscopy with a fine time resolution. We assessed its advantage over the traditional step-scan method by performing time-resolved spectroscopy using each method. The fast-scan pump-probe system can perform measurements within 2 min. The results show higher reproducibility and reliability than those obtained by the step-scan method.
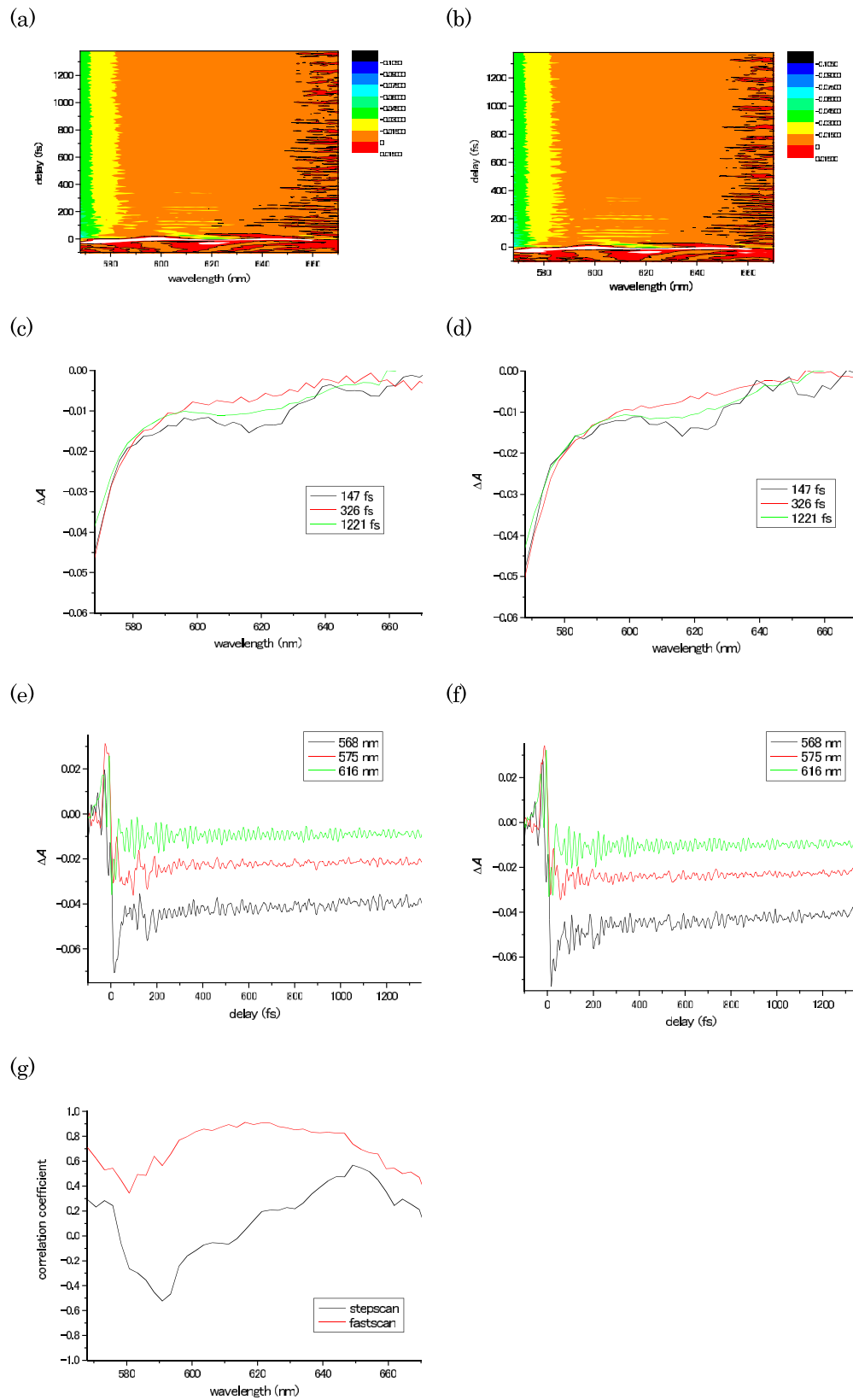
FIG. 6. (Color online) ΔA traces obtained by the fast-scan method for delay times of (a) -390 to 1396 fs, and (b) 1396 to -390 fs. Time-resolved ΔA spectra at delays of 147, 326, and 1221 fs are plotted in (c) and (d), and ΔA traces at 568, 575, and 616 nm are plotted in (e) and (f). (g) Correlation coefficient between the time traces of the forward and backward scans from 150 to 1350 fs for the step-scan and fast-scan measurements.

APPENDIX A: NOPA

The source laser is a regenerative chirped pulse amplifier (Coherent Legend-USP) seeded with a fiber laser oscillator. The amplifier generates femtosecond pulses whose duration, central wavelength, repetition rate, and average power are 40 fs, 800 nm, 5 kHz, and 2.5 W, respectively. The NOPA uses a phase-matching condition to generate amplified visible pulses with a broad spectral width of 200 THz. Angular dis-
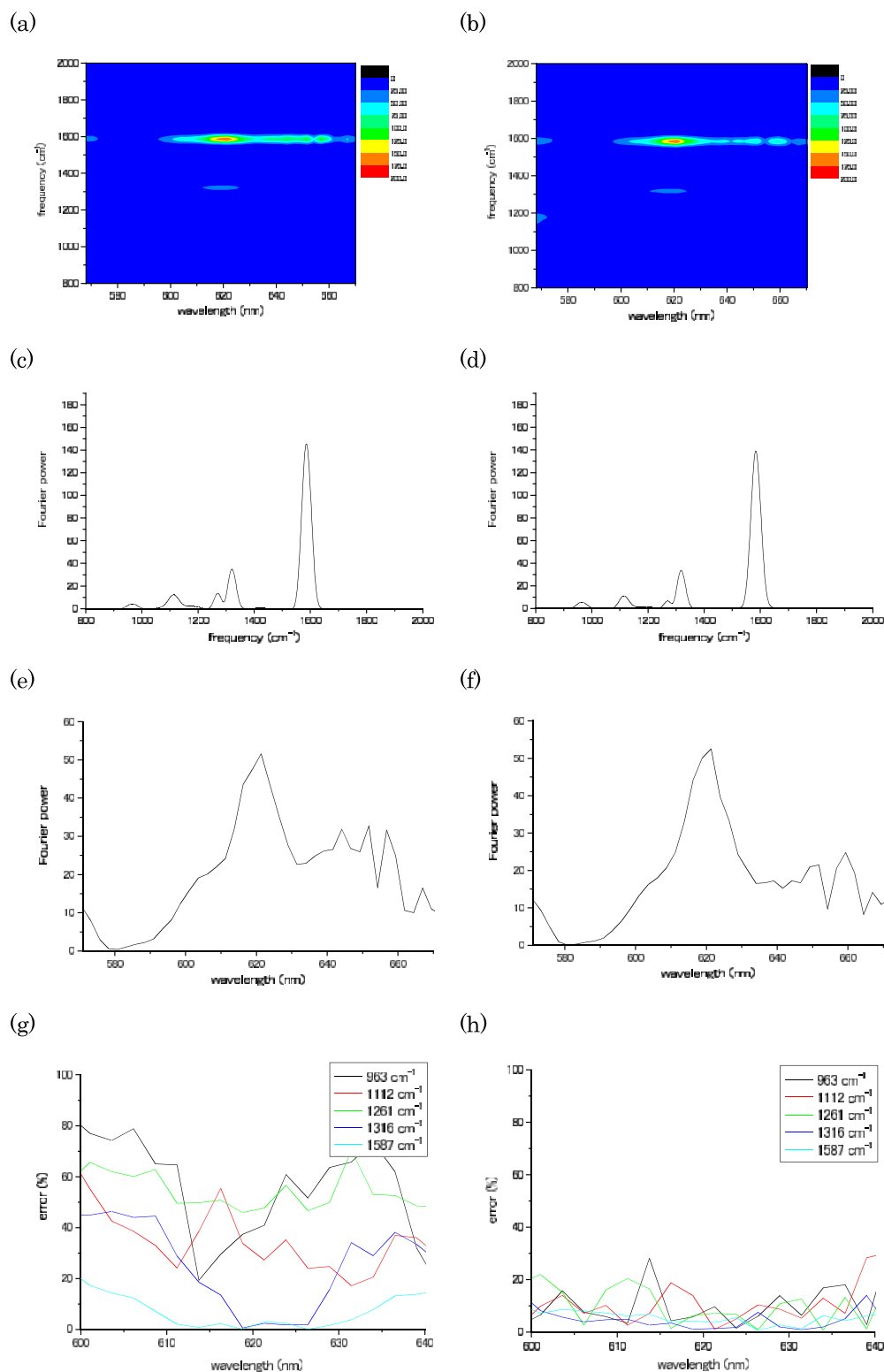
FIG. 7. (Color online) (a) and (b) are Fourier power spectra of the ΔA traces from Figs. 6(a) and 6(b), respectively. Fourier power spectra at 616 nm are plotted in (c) and (d). Fourier power spectra of the most prominent vibrational mode at 1588 cm^{-1} are graphed in (e) and (f). Errors in five vibrational mode intensities for step-scan and fast-scan measurements are shown in (g) and (h).

persion of the pump beam (introduced by a Brewster prism) also contributes to broadening the spectral width of the pulses. The time duration of the pump pulses was stretched to decrease their peak intensity and to avoid damaging the optical components. A long duration of the pump pulses also helps reduce sensitivity to timing drifts, which improve the power stability of the broadband output.

The spectral width of the output pulses is large enough to generate sub-10-fs laser pulses. For time-resolved spectroscopy, it is necessary to use ultrashort laser pulses to resolve real-time molecular vibrations. Consequently the broadband visible laser pulses were compressed using two dielectric broadband chirped mirrors, a 300 lines/mm diffraction grating in negative first order, and a 200 mm radius
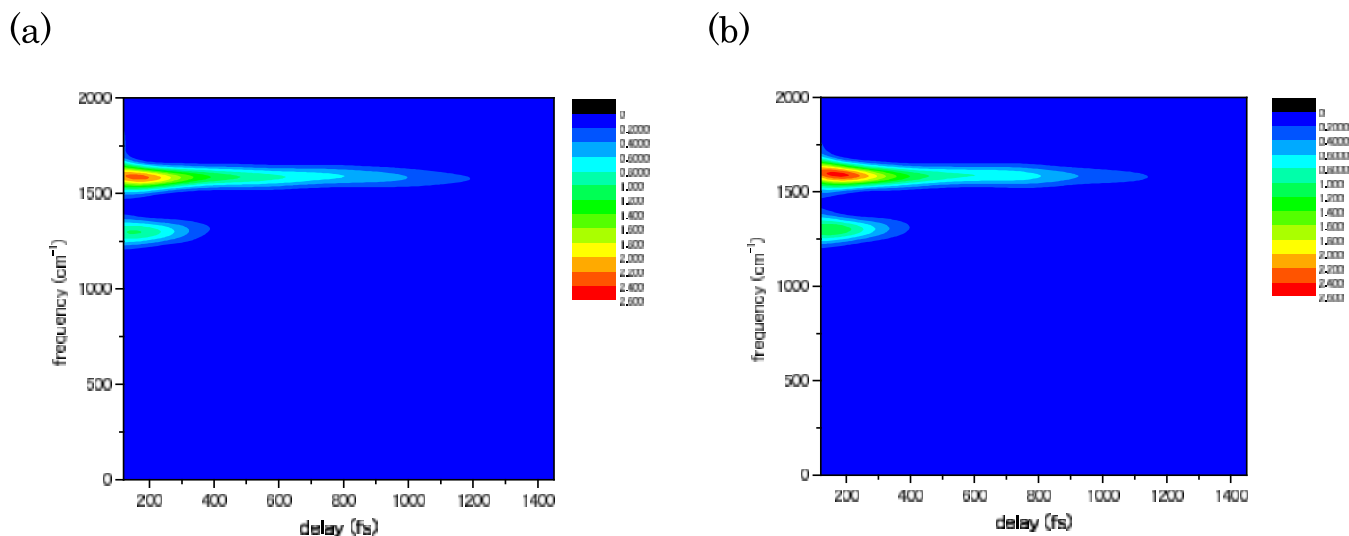
(a)

(b)

FIG. 8. (Color online) (a) and (b) Spectrograms calculated form the time-resolved ΔA traces at 616 nm plotted in Figs. 6(e) and 6(f).

spherical mirror with a flexible mirror positioned in its focal plane. A horizontal grating angle was used for crude compression of the pulse width. To fine tune the pulse compression, the voltages applied to the piezoelectric array behind the flexible mirror were adjusted over a tuning range of 6 μm. During the tuning process, the character of the ultrashort pulses was monitored to guide the alignment procedure, using the SHG frequency-resolved optical gating (FROG) technique. Feedback is provided to the piezoelectric array behind the flexible mirror. A translation stage (SIGMA TECH model STC-1020X), with a built-in interferometer and active position stabilization, is used to obtain a position accuracy of 10 nm. It was used in the FROG apparatus for both wide- and narrow-range delay scans. Two identical 2-μm-thick pellicle beamsplitters, which have flat reflectivity across the visible spectral range, were used to balance the dispersion in the two beams of the FROG apparatus. Both beams were focused onto a wedged ultrathin β-BaB$_2$O$_4$ crystal for broadband SHG and were collimated behind it using a 200 mm off-axis parabolic mirror. The thickness of the wedge varied across the face of the crystal between 5 and 20 μm. By observing the spectral phase in the SHG FROG measurement, chirp compensation was performed by adjusting the 38 actuators of the flexible mirror (lined up in two rows that provide a clear aperture of 39×11 mm^2).

The broadband visible laser pulses were compressed to resolve real-time molecular vibrations whose frequencies are lower than 3000 cm^{-1}. The setup of the SHG FROG measurement system is identical to that of the time-resolved pump-probe system used for the molecular vibrational analysis. Therefore, the SHG FROG setup was also used for the measurement of the time-resolved pump-probe signals. The thin beamsplitters used for the SHG FROG measurement divided the compressed ultrashort visible laser pulses into pump and probe beams.

APPENDIX B: SAMPLE FILM

A poly[2-methoxy-5-(20-ethyl-hexyloxy)-p-phenylene vinylene] (MEH-PPV) film was used for pump-probe measurements. It was prepared by spin coating chloroform solu-

tions of MEH-PPV onto quartz plates to form 0.5–1.0 μm thick films. An absorption spectrum of the MEH-PPV film is shown in Fig. 1, recorded using a scanning spectrophotometer (UV-3101PC from Shimadzu). All measurements were performed at room temperature (295 ± 1 K).

[1] M. J. Feldstein, P. Vohringer, and N. F. Scherer, J. Opt. Soc. Am. B **12**, 1500 (1995).
[2] F. Pellegrino, Opt. Eng. **22**, 508 (1983).
[3] A. B. Rubin, L. B. Rubin, V. Z. Pashchenko, A. A. Kononenko, and B. A. Gulyaev, Kvantovaya Elektron. (Kiev) **7**, 52 (1980).
[4] M. R. Wasielewski, P. A. Liddell, D. Barrett, T. A. Moore, and D. Gust, Nature (London) **322**, 570 (1986).
[5] A. Boyer, M. Dery, P. Selles, C. Arbour, and F. Boucher, Biosens. Bioelectron. **10**, 415 (1995).
[6] K. J. Hellingwerf, J. Hendriks, and T. Gensch, J. Biol. Phys. **28**, 395 (2002).
[7] Y. Imamoto and M. Kataoka, Photochem. Photobiol. **83**, 40 (2007).
[8] G. Eichmann, Y. Li, and R. R. Alfano, Opt. Eng. **25**, 91 (1986).
[9] D. J. Olego, R. Schachter, M. Viscogliosi, and L. A. Bunz, Appl. Phys. Lett. **49**, 719 (1986).
[10] C. P. Singh, K. S. Bindra, B. Jain, and S. M. Oak, Opt. Commun. **245**, 407 (2005).
[11] L. Kuhnert, Nature (London) **319**, 393 (1986).
[12] S. Tazuke, Solid State Phys. **23**, 61 (1988).
[13] N. E. Korolev, I. Y. Mokienko, A. E. Poletimov, and A. S. Shcheulin, Phys. Solid State **127**, 327 (1991).
[14] A. H. Zewail, Science **242**, 1645 (1988).
[15] R. M. Bowman, M. Dantus, and A. H. Zewail, Chem. Phys. Lett. **156**, 131 (1989).
[16] M. Gruebele, I. R. Sims, E. D. Potter, and A. H. Zewail, J. Chem. Phys. **95**, 7763 (1991).
[17] M. Dantus and A. H. Zewail, Chem. Rev. **104**, 1717 (2004).
[18] A. Baltuska, Z. Wei, M. S. Pshenichnikov, and D. A. Wiersma, Opt. Lett. **22**, 102 (1997).
[19] M. Nisoli, S. De Silvestri, O. Svelto, R. Szipocs, K. Ferencz, Ch. Spielmann, S. Sartania, and F. Krausz, Opt. Lett. **22**, 522 (1997).
[20] A. Shirakawa, I. Sakane, and T. Kobayashi, Opt. Lett. **23**, 1292 (1998).
[21] G. Cerullo, M. Nisoli, S. Stagira, and S. De Silvestri, Opt. Lett. **23**, 1283 (1998).
[22] M. Adachi, K. Yamane, R. Morita, and M. Yamashita, Jpn. J. Appl. Phys., Part 1 **44**, 4123 (2005).
[23] A. Baltuška, T. Fuji, and T. Kobayashi, Opt. Lett. **27**, 306 (2002).
[24] A. Shirakawa and T. Kobayashi, Appl. Phys. Lett. **72**, 147 (1998).
[25] A. Shirakawa, I. Sakane, M. Takasaka, and T. Kobayashi, Appl. Phys. Lett. **74**, 2268 (1999).
[26] A. Baltuška, M. F. Emde, M. S. Pshenichnikov, and D. A. Wiersma, J. Phys. Chem. A **103**, 10065 (1999).

[27] G. Cerullo, G. Lanzani, M. Muccini, C. Taliani, and S. De Silvestri, Phys. Rev. Lett. **83**, 231 (1999).

[28] R. A. G. Cinelli, V. Tozzini, V. Pellegrini, F. Beltram, G. Cerullo, M. Zavelani-Rossi, S. D. Silvestri, M. Tyagi, and M. Giacca, Phys. Rev. Lett. **86**, 3439 (2001).

[29] W. T. Pollard, S.-Y. Lee, and R. A. Mathies, J. Chem. Phys. **92**, 4012 (1990).

[30] T. Kobayashi, T. Saito, and H. Ohtani, Nature (London) **414**, 531 (2001).

[31] T. Taneichi, T. Fuji, Y. Yuasa, and T. Kobayashi, Chem. Phys. Lett. **394**, 377 (2004).

[32] A. Colonna, A. Yabushita, I. Iwakura, and T. Kobayashi, Chem. Phys. **341**, 336 (2007).

[33] A. Yabushita and T. Kobayashi, Biophys. J. **96**, 1447 (2009).

[34] T. Kobayashi, I. Iwakura, and A. Yabushita, New J. Phys. **10**, 065016 (2008).

[35] G. Cerullo, G. Lanzani, L. Pallaro, and S. De Silvestri, J. Mol. Struct. **521**, 261 (2000).

[36] T. Cimei, A. R. Bizzarri, G. Cerullo, S. De Silvestri, and S. Cannistraro, Biophys. Chem. **106**, 221 (2003).

[37] A. Gambetta, C. Manzoni, E. Menna, M. Meneghetti, G. Cerullo, G. Lanzani, S. Tretiak, A. Piryatinski, A. Saxena, R. L. Martin, and A. R. Bishop, Nat. Phys. **2**, 515 (2006).

[38] T. P. Nguyen, S. H. Yang, P. Le Rendu, and H. Khan, Composites, Part A **36**, 515 (2005).